Kinetic Study of the Reactions of BrO Radicals with HO_2 and DO_2

Yuri Bedjanian,* Véronique Riffault, and Gilles Poulet†

Laboratoire de Combustion et Systèmes Réactifs, CNRS, and Université d'Orléans, 45071 Orléans Cedex 2, France

Received: September 13, 2000; In Final Form: January 17, 2001

The kinetics of the reactions of BrO radicals with HO_2 and DO_2 radicals, $HO_2 + BrO \rightarrow$ products (1) and $DO_2 + BrO \rightarrow$ products (3), have been studied by the mass spectrometric discharge flow method at temperatures between 230 and 360 K and at a total pressure of 1 Torr of helium. The rate constant of reaction 1 as determined by monitoring either the HO_2 or the BrO decay (in excess of BrO or HO_2, respectively) is given by the Arrhenius expression $k_1 = (9.4 \pm 2.3) \times 10^{-12} \exp[(345 \pm 60)/T]$ cm^3 molecule^{-1} s^{-1}, with $k_1 = (3.1 \pm 0.8) \times 10^{-11}$ cm^3 molecule^{-1} s^{-1} at $T = 298$ K, where the uncertainties represent 95% confidence limits and include estimated systematic errors. The rate constant of reaction 3, measured under pseudo-first-order conditions in an excess of BrO, is $k_3 = (3.9 \pm 1.2) \times 10^{-12} \exp[(410 \pm 80)/T]$ cm^3 molecule^{-1} s^{-1}, with $k_3 = (1.6 \pm 0.4) \times 10^{-11}$ cm^3 molecule^{-1} s^{-1} at $T = 298$ K, where the uncertainties represent 95% confidence limits and include estimated systematic errors. The value of k_3 was measured for the first time, whereas the value of k_1 was compared with those from previous studies. From the observation that no ozone formed among the products of the $HO_2 + BrO$ reaction, an upper limit was derived for the channel $HO_2 + BrO \rightarrow HBr + O_3$ (1b) of reaction 1: $k_{1b}/k_1 < 0.004$ at $T = 298$ K. The implication of this result for stratospheric bromine partitioning is briefly discussed.

Introduction

The reaction between HO_2 and BrO radicals can follow two possible channels:

$$HO_2 + BrO \rightarrow HOBr + O_2 \quad (1a)$$

$$\rightarrow HBr + O_3 \quad (1b)$$

The major reaction pathway (1a) has been recognized as one of the key stratospheric bromine processes, as it is a rate-limiting step in the following catalytic cycle of ozone destruction:[1,2]

$$\begin{aligned} &Br + O_3 \rightarrow BrO + O_2 \\ &BrO + HO_2 \rightarrow HOBr + O_2 \quad (1a) \\ &HOBr + h\nu \rightarrow Br + OH \\ &OH + O_3 \rightarrow HO_2 + O_2 \\ &\text{---------------------} \\ &2O_3 \rightarrow 3O_2 \end{aligned}$$

The second reaction channel (1b) is of potential importance for the stratospheric chemistry of bromine. The existence of this pathway might significantly influence the overall partitioning of bromine in the stratosphere and, thus, might also affect bromine-catalyzed ozone loss (e.g., ref 3).

Reaction 1 has been studied in a number of laboratories.[2,4−9] The first measurements, by Cox and Sheppard[4] using modulated photolysis and molecular modulation/UV−visible absorption as the detection method, led to the value $k_1 = 0.5^{+0.5}_{-0.3} \times 10^{-11}$ cm^3 molecule^{-1} s^{-1} at 303 K and atmospheric pressure. Much higher values of k_1, $(3.3 \pm 0.5) \times 10^{-11}$ and $(3.4 \pm 1.0) \times 10^{-11}$ cm^3 molecule^{-1} s^{-1}, were measured by Poulet et al.[2] employing discharge flow reactor and mass spectrometry techniques and by Bridier et al.[5] with a flash photolysis/UV−visible absorption method, respectively. Reaction 1 was revisited by Orléans group in ref 6, where the temperature dependence of the rate constant at $T = 233-344$ K was reported for the first time: $k_1 = (4.8 \pm 0.3) \times 10^{-12} \exp[(580 \pm 100)/T]$ cm^3 molecule^{-1} s^{-1}. Results from two more recent temperature dependence studies,[7,8] also carried out in a discharge flow reactor combined with a mass spectrometer (chemical ionization[7] and electron impact[8]), confirmed the negative temperature dependence of k_1, observed in ref 6, with the activation factors $E/R = (520 \pm 80)$[7] and (540 ± 210) K.[8] Although the activation energies agree well, significantly lower values of k_1 at room temperature were reported in these studies: $k_1 = (1.4 \pm 0.3) \times 10^{-11}$ by Elrod et al.[7] and $k_1 = (1.7 \pm 0.6) \times 10^{-11}$ (with an excess of HO_2) and $(2.1 \pm 0.6) \times 10^{-11}$ (with BrO in excess) by Li et al.[8] Finally, the most recent study of Cronkhite et al.,[9] where the rate constant of reaction 1 was measured using laser flash photolysis/UV absorption (for BrO detection)/IR tunable diode laser absorption (for HO_2 detection), led to $k_1 = (2.0 \pm 0.6) \times 10^{-11}$ cm^3 molecule^{-1} s^{-1} at $T = 296$ K, thus supporting a smaller rate coefficient for reaction 1. The existing discrepancy (of around a factor of 2) in the available room-temperature data for k_1 is one of the motivations for the present reinvestigation of reaction 1, which was studied at $T = 230-360$ K using different sources of radicals over a wide range of experimental conditions.

The data on the branching ratio for the minor HBr-forming channel of reaction 1 have been reported in only two studies.[6,10] From the investigation of the reverse reaction, $HBr + O_3 \rightarrow HO_2 + BrO$, Mellouki et al.[10] estimated an upper limit for the branching ratio of the channel (1b): $k_{1b}/k_1 < 0.0001$ at $T =$

* Corresponding author. E-mail: bedjanian@cnrs-orleans.fr.

† Now at CNRS−LPCE (Laboratoire de Physique et Chimie de l'Environnement), Orléans, France.

10.1021/jp0032255 CCC: $20.00
Published on Web 02/24/2001

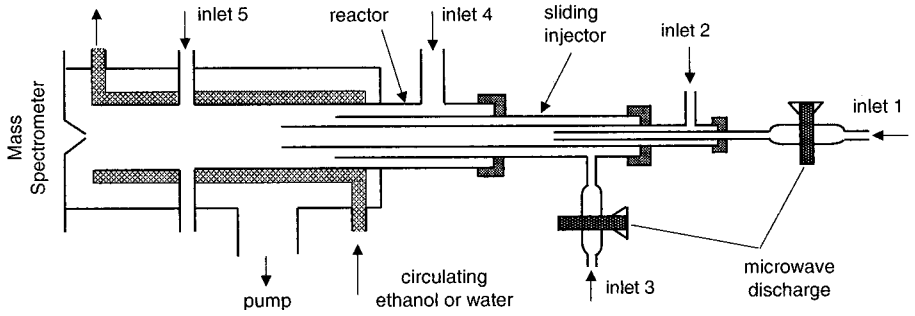

Figure 1. Diagram of the apparatus used (see text).

300 K. In the unique direct experimental determination of this branching ratio, an upper limit of 0.015 was derived at $T = 233-300$ K from the absence of detection of O_3 in the products of reaction 1.[6] However, recent model calculations[3] have shown that a branching ratio even as low as 0.01 for the HBr + O_3 forming channel of reaction 1 could lead to a reasonable agreement between observed and calculated stratospheric HBr profiles. In the present study, an attempt has been made to verify experimentally the possible existence of a 1% yield of HBr and O_3 for reaction 1.

Our present study of the BrO + $HO_2(DO_2)$ reactions is an integral step in our current investigation of the OH(OD) + BrO reaction, as it will allow us to quantify the influence of secondary chemistry on these reactions. This will better enable us to accurately measure the HBr yield from the reaction

$$OH + BrO \rightarrow HO_2 + Br \quad (2a)$$

$$\rightarrow HBr + O_2 \quad (2b)$$

Similarly to reaction 1b, the potential occurrence of channel 2b is of importance for stratospheric bromine partitioning,[3,11] although the branching ratio for this channel is expected to be very low (a maximum of a few percent). The determination of the total rate constant for reaction 2 also represents a significant experimental challenge, as it is difficult to avoid the influence of multiple possible secondary and side processes involving reactants and products of reaction 2 as well as the species used to produce OH and BrO radicals.[12] Thus, all of these processes should be well characterized. The reaction of BrO with the major product of reaction 2, HO_2 radicals, is one of these processes. The detection of small yields of HBr from the OH + BrO reaction is also an experimental problem, as relatively high residual concentrations of HBr are known to be present in bromine-containing chemical systems used in the laboratory. In this respect, the reaction OD + BrO, the isotopic analogue of reaction 2, seems to be more appropriate for the determination of the DBr yield (which is expected to be similar to the HBr yield from OH + BrO reaction). However, in this case, accurate kinetic data on the relevant reactions of OD and DO_2 radicals, including reaction 3, (which are very scarce) are needed. In previous papers from this laboratory, the kinetic data for the reactions OH(OD) + OH(OD),[13] OH(OD) + Br_2,[14] OH(OD) + HBr(DBr),[15] and Br + $HO_2(DO_2)$[16] have been reported. Together with the study of reaction 1, the present work reports the measurements of the rate constant for reaction 3 over the temperature range 230−360 K

$$BrO + DO_2 \rightarrow \text{products} \quad (3)$$

Experimental Section

Experiments were carried out in a discharge flow reactor using a modulated molecular beam mass spectrometry as the detection method. The main reactor, shown in Figure 1 along with the movable injector for the reactants, consisted of a Pyrex tube (45 cm length and 2.4 cm i.d.) with a jacket for the thermostated liquid circulation (water or ethanol). The walls of the reactor, as well as those of the injector, were coated with halocarbon wax to minimize the heterogeneous loss of active species. All experiments were conducted at 1 Torr total pressure, with helium being used as the carrier gas.

The following two reactions were used to produce BrO radicals:

$$O + Br_2 \rightarrow BrO + Br \quad (4)$$

$$k_4 = 1.8 \times 10^{-11} \exp(40/T) \text{ cm}^3 \text{ molecule}^{-1} \text{ s}^{-1}$$ [17]

$$Br + O_3 \rightarrow BrO + O_2 \quad (5)$$

$$k_5 = 1.7 \times 10^{-11} \exp(-800/T) \text{ cm}^3 \text{ molecule}^{-1} \text{ s}^{-1}$$ [18]

O atoms were generated from the microwave discharge of O_2/He mixtures. Br atoms were produced either from the microwave discharge of Br_2/He mixtures or from reaction 4 between O atoms and Br_2. BrO radicals were detected at their parent peaks at $m/e = 95$ and $m/e = 97$ as BrO^+.

The fast reaction of fluorine atoms with H_2O_2 was used as the source of HO_2 radicals, with F atoms being produced from the microwave discharge of F_2/He mixtures.

$$F + H_2O_2 \rightarrow HO_2 + HF \quad (6)$$

$$k_6 = 5.0 \times 10^{-11} \text{ cm}^3 \text{ molecule}^{-1} \text{ s}^{-1} \ (T = 300 \text{ K})$$ [19]

It was verified by mass spectrometry that more than 90% of the F_2 was dissociated in the microwave discharge. To reduce F-atom reactions with the glass surface inside the microwave cavity, a ceramic (Al_2O_3) tube was inserted in this part of the injector. Similarly, the reaction of F atoms with D_2O_2 was used to produce DO_2 radicals.

$$F + D_2O_2 \rightarrow DO_2 + DF \quad (7)$$

H_2O_2 and D_2O_2 were always used in excess over F atoms.

This source of $HO_2(DO_2)$ radicals is known to produce active species other than $HO_2(DO_2)$. First, OH(OD) radicals can be formed in the reaction of F atoms with $H_2O(D_2O)$ (from the H_2O_2 and D_2O_2 solutions).

$$F + H_2O \rightarrow OH + HF \quad (8)$$

$$k_8 = 1.4 \times 10^{-11} \exp[(0 \pm 200)/T] \text{cm}^3 \text{ molecule}^{-1} \text{ s}^{-1}$$ [18]

$$F + D_2O \rightarrow OD + DF \quad (9)$$

Second, another active species that can enter the reactor is O

atoms, coming from either the discharge of F_2 or the secondary reaction $F + OH \rightarrow O + HF$. However, the concentrations of the above-mentioned trace species can easily be measured using an addition of Br_2 into the reactor by the following method. Br_2, being inert toward $HO_2(DO_2)$ radicals, removes all other trace active species coming from the source of $HO_2(DO_2)$, i.e., OH(OD), O, and F [if not completely consumed in reaction with $H_2O_2(D_2O_2)$] via the fast reactions 4, 10, 11, and 12.

$$OH + Br_2 \rightarrow Br + HOBr \quad (10)$$

$$k_{10} = 1.8 \times 10^{-11}\exp(235/T)\ \text{cm}^3\ \text{molecule}^{-1}\ \text{s}^{-1}$$ [14]

$$OD + Br_2 \rightarrow Br + DOBr \quad (11)$$

$$k_{11} = 1.9 \times 10^{-11}\exp(220/T)\ \text{cm}^3\ \text{molecule}^{-1}\ \text{s}^{-1}$$ [14]

$$F + Br_2 \rightarrow FBr + Br \quad (12)$$

$$k_{12} = 2.2 \times 10^{-10}\ \text{cm}^3\ \text{molecule}^{-1}\ \text{s}^{-1}\ (T = 300\ \text{K})$$ [20]

The concentrations of these trace species can easily be measured using the mass spectrometric detection of HOBr(DOBr), BrO, and FBr, which are products.

The HO_2 and DO_2 radicals were detected at their parent peaks at $m/e = 33$ (HO_2^+) and $m/e = 34$ (DO_2^+). These signals were always corrected for the contribution of H_2O_2 and D_2O_2 due to their fragmentation in the ion source, which was operating at 25−30 eV. These corrections could easily be made by simultaneous detection of the signals from H_2O_2 at $m/e = 33$ and 34 ($m/e = 34$ and 36 for D_2O_2). Additional signals at $m/e = 33$ and 34 were observed because of oxygen isotope ions $O^{16}O^{17+}$ ($m/e = 33$) and $O^{17}O^{17+}$ ($m/e = 34$) when high O_3 (O_2) concentrations were introduced into the reactor. This contribution was also easily measured by detecting the signals at $m/e = 33$ and 34 in the absence of $H_2O_2/HO_2(D_2O_2/DO_2)$ in the reactor.

The determination of the absolute concentrations of the labile species is one of the major sources of uncertainty in measurements of the rate constants for radical−radical reactions. In the present study, two methods were used for the determination of the absolute concentrations of BrO radicals. The first consisted of the usually used procedure of BrO titration with NO with the subsequent detection of NO_2 formed ($[BrO] = [NO_2]$).

$$BrO + NO \rightarrow Br + NO_2 \quad (13)$$

$$k_{13} = 8.8 \times 10^{-12}\exp(260/T)\ \text{cm}^3\ \text{molecule}^{-1}\ \text{s}^{-1}$$ [18]

In this case, BrO was formed in reaction 4 in order to avoid the regeneration of BrO through reaction 5 if O_3 was present in the reactor. Another method for the calibration of BrO signals employed reaction 5 between Br atoms and ozone. Br atoms, formed in the microwave discharge of Br_2, were consumed by high concentrations of O_3 ($[O_3] \approx 10^{15}$ molecule cm^{-3}). The concentration of BrO was then determined from the fraction of Br_2 dissociated in the microwave discharge. During these calibration experiments, the influence of the recombination reaction of BrO radicals (14) (leading to a steady state for [Br]) was negligible because of the high ozone concentrations used.

$$BrO + BrO \rightarrow Br + Br + O_2 \quad (14a)$$

$$\rightarrow Br_2 + O_2 \quad (14b)$$

$$k_{14} = 1.5 \times 10^{-12}\exp(230/T)\ \text{cm}^3\ \text{molecule}^{-1}\ \text{s}^{-1}$$ [18]

$$k_{14a}/k_{14} = 1.6 \times \exp(-190/T)$$ [18]

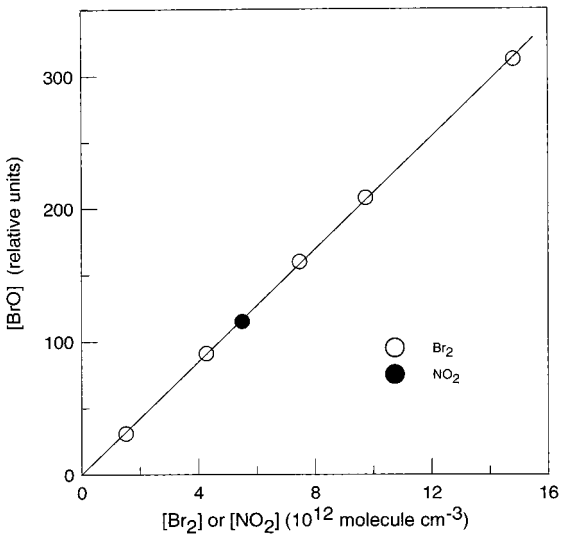

Figure 2. Example of calibration curve for BrO: dependencies of the concentration of BrO consumed in reaction 13 on the concentration of NO_2 formed and of the concentration of BrO formed in reaction 5 on the concentration of Br_2 consumed (see text).

In addition, all bromine-containing species involved in reactions 5 and 14 were detected, and the small concentrations of Br atoms (not transformed to BrO) could be measured and taken into account through the relation $2\Delta[Br_2] = [BrO] + [Br]$, where $\Delta[Br_2]$ is the fraction of Br_2 dissociated in the discharge. An example of the BrO calibration curve obtained using these two approaches is shown in Figure 2. The absolute concentrations of BrO determined by these different methods were always in good agreement (within a few percent).

The absolute concentrations of HO_2 were measured using the chemical conversion of HO_2 to the stable species NO_2 through reaction 15.

$$HO_2 + NO \rightarrow OH + NO_2 \quad (15)$$

$$k_{15} = 3.5 \times 10^{-12}\exp(250/T)\ \text{cm}^3\ \text{molecule}^{-1}\ \text{s}^{-1}$$ [18]

Reaction 15 leads to the production of OH radicals, which can regenerate HO_2 through reaction 16.

$$OH + H_2O_2 \rightarrow HO_2 + H_2O \quad (16)$$

$$k_{16} = 2.9 \times 10^{-12}\exp(-160/T)\ \text{cm}^3\ \text{molecule}^{-1}\ \text{s}^{-1}$$ [18]

To prevent this possible HO_2 regeneration, the calibration experiments were carried out in the presence of Br_2, which rapidly scavenged OH through reaction 10, forming HOBr. An example of the HO_2 calibration curve is shown in Figure 3. Assuming stoichiometric conversions of HO_2 to NO_2 (OH) and of OH to HOBr, one can derive the relation $[HO_2] = [NO_2] = [HOBr]$, which also means that the HO_2 concentration can be measured through the detection of HOBr. This possibility was investigated, and the concentrations of HO_2 determined through $[NO_2]$ and [HOBr] measurements were found to be in agreement to within 10%. The absolute concentrations of HOBr were measured using the reaction of OH radicals with excess Br_2 (reaction 10). OH radicals were formed through the fast reaction of H atoms with excess NO_2.

$$H + NO_2 \rightarrow OH + NO \quad (17)$$

$$k_{17} = 4 \times 10^{-10}\exp(-340/T)\ \text{cm}^3\ \text{molecule}^{-1}\ \text{s}^{-1}$$ [18]

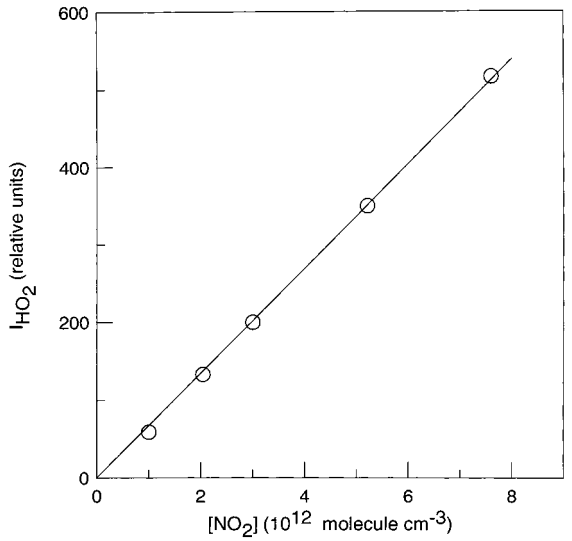

Figure 3. Example of calibration curve for HO_2: dependence of the concentration of HO_2 consumed in reaction 15 on the concentration of NO_2 formed (see text).

Thus, HOBr concentrations were determined from the consumed concentration of Br_2: $[OH] = [HOBr] = \Delta[Br_2]$. The possible influence of secondary chemistry on this procedure for the absolute calibration of the HOBr (and OH) signals was discussed in detail in previous papers.[13,14] A similar procedure was employed for the measurement of the absolute concentrations of DO_2 radicals. The H_2O_2 calibration method, consisting of the titration of H_2O_2/H_2O by an excess of F atoms, was also described in a previous paper.[16] The absolute concentrations of ozone were derived using the reaction between O_3 and NO with detection and calibration of the NO_2 formed ($\Delta[O_3] = \Delta[NO_2]$).

$$NO + O_3 \rightarrow NO_2 + O_2 \qquad (18)$$

$$k_{18} = 2 \times 10^{-12} \exp(-1400/T)\ \text{cm}^3\ \text{molecule}^{-1}\ \text{s}^{-1}\ ^{18}$$

The concentrations of other stable species in the reactor were calculated from their flow rates, which were obtained from measurements of the pressure drop in calibrated volume flasks containing mixtures of the species with helium.

The purities of the gases used were as follows: He, >99.9995% (Alphagaz), was passed through liquid nitrogen traps; H_2, >99.998% (Alphagaz); Br_2, >99.99% (Aldrich); F_2, 5% in helium (Alphagaz); NO_2, >99% (Alphagaz); and NO, >99% (Alphagaz), purified by trap-to-trap distillation to remove NO_2 traces. A 70% H_2O_2 solution was purified to around 90% by flowing helium through the bubbler with H_2O_2. Ozone was produced by an ozonizer (Trailigaz) and was collected and stored in a trap containing silica gel at $T = 195$ K. The trap was pumped before use to reduce the O_2 concentration. The resulting oxygen concentration was always lower than 20% of the ozone concentration introduced into the reactor.

Results

Rate Constant for the BrO + HO_2 Reaction. Three series of experiments were performed to measure the rate constant for the reaction BrO + HO_2. The rate constant of reaction 1 was determined (i) from the monitoring of the HO_2 consumption kinetics in an excess of BrO, (ii) from the monitoring of the BrO decays in an excess of HO_2 radicals, and (iii) from relative rate measurements using the reaction of Br atoms with HO_2 as the reference reaction.

TABLE 1: Reaction HO_2 + BrO → HOBr + O_2 (1): Experimental Conditions and Results

N/exp[a]	T (K)	$[HO_2]$[b]	[BrO][b]	k_1[c]	excess reactant
9	360	0.5−1.1	0.6−14.3	2.4 ± 0.2	BrO
9	320	0.3−6.0	0.2−0.3	2.7 ± 0.2	HO_2
14	298	0.5−7.0	0.2−0.4	3.2 ± 0.2	HO_2
15	297	0.6−1.3	0.8−13.5	3.0 ± 0.1	BrO
10	275	0.3−6.9	0.2−0.3	3.2 ± 0.1	HO_2
8	263	0.5−1.0	0.6−10.2	3.6 ± 0.2	BrO
7	250	1.3−8.9	0.3−0.4	3.7 ± 0.3	HO_2
7	243	0.5−1.1	0.7−9.1	3.8 ± 0.2	BrO
8	240	0.4−4.2	0.2−0.4	3.9 ± 0.2	HO_2
8	230	0.6−4.3	0.2−0.4	4.2 ± 0.2	HO_2

[a] Number of kinetic runs. [b] Concentrations are in units of 10^{12} molecule cm^{-3}. [c] Rate constants are in units of 10^{-11} cm^3 $molecule^{-1}$ s^{-1}; the error represents $\pm 2\sigma$.

$$Br + HO_2 \rightarrow HBr + O_2 \qquad (19)$$

$$k_{19} = 4.9 \times 10^{-12} \exp(-310/T)\ \text{cm}^3\ \text{molecule}^{-1}\ \text{s}^{-1}\ ^{16}$$

BrO Kinetics in Excess HO_2. In this series of experiments, the BrO decay kinetics were monitored in the presence of an excess concentration of HO_2. HO_2 radicals were formed through reaction 6, with F atoms being introduced into the reactor through inlet 3 (see Figure 1) and H_2O_2 molecules through the sidearm of the reactor (inlet 4). BrO radicals were formed in the central tube of the movable injector by reaction of oxygen atoms (inlet 1) with excess Br_2 (inlet 2). The initial concentrations of the reactants, HO_2 and BrO radicals, are shown in Table 1. Concentrations of the excess precursor species, Br_2 and H_2O_2, were in the ranges $(5-7) \times 10^{13}$ and $(1-6) \times 10^{13}$ molecule cm^{-3}, respectively. The presence of relatively high concentrations of Br_2 in the reactor allowed for a rapid scavenging of all active trace species from the source of HO_2 (see previous section), thus preventing their possible reactions with BrO. This was important, especially for the suppression of the fast reaction 2 of OH radicals with BrO, which could contribute to the observed BrO decays, since a high rate constant at room temperature was determined by Bogan et al. in the one study of this reaction: $k_2 = (7.5 \pm 4.2) \times 10^{-11}$ cm^3 $molecule^{-1}$ s^{-1}.[12] One can note that the value of k_2 determined in preliminary experiments from this laboratory is lower by a factor of 2. The flow velocity in the reactor was in the range 1460−2010 cm s^{-1}. The concentrations of both BrO and HO_2 radicals were measured simultaneously as a function of the reaction time. The consumption of the excess reactant, HO_2, was also observed (up to 30% in a few kinetic runs). This HO_2 consumption was due to reaction 1, to the wall loss of HO_2 radicals, to reaction 19 (with Br atoms from the BrO source), and to HO_2 disproportionation (reaction 20).

$$HO_2 + HO_2 \rightarrow H_2O_2 + O_2 \qquad (20)$$

$$k_{20} = 2.3 \times 10^{-13} \exp(600/T)\ \text{cm}^3\ \text{molecule}^{-1}\ \text{s}^{-1}\ ^{18}$$

This HO_2 consumption was taken into account using the mean HO_2 concentration along the BrO decay. It was verified that the results obtained in this way for k_1 were consistent (within 5%) with those derived from the fitting of the BrO decay kinetics using the experimentally measured HO_2 profiles. Examples of kinetic runs of the exponential decay of [BrO] measured with various excess concentrations of HO_2 radicals are shown in Figure 4. The pseudo-first-order rate constants, $k_1' = -$d(ln-

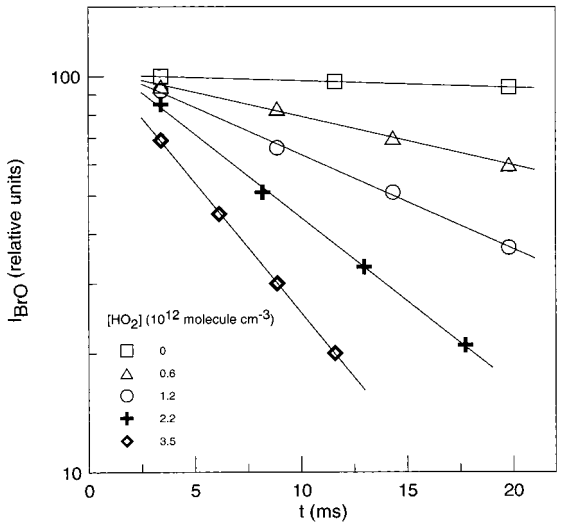

Figure 4. Reaction $HO_2 + BrO \rightarrow HOBr + O_2$ (1): examples of experimental BrO decay kinetics monitored in excess HO_2 at $T = 230$ K.

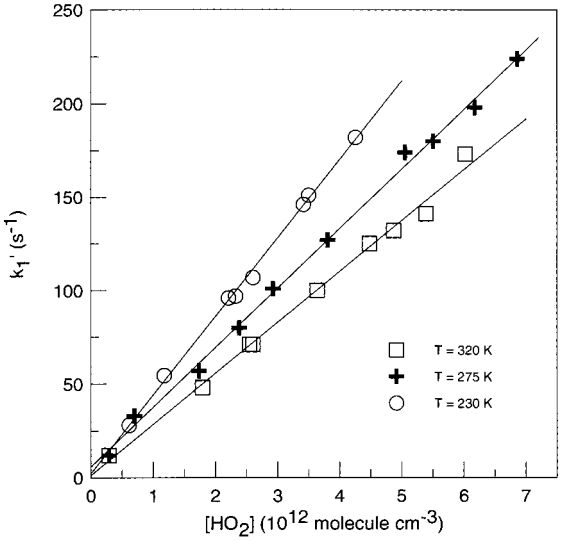

Figure 5. Reaction $HO_2 + BrO \rightarrow HOBr + O_2$ (1): examples of pseudo-first-order plots obtained from BrO decay kinetics in excess HO_2 at different temperatures.

[BrO])/dt, were corrected for the axial and radial diffusion of BrO.[21] The diffusion coefficient of BrO in He was calculated from that of Kr in He[23] and varied from 0.42 cm^2 s^{-1} at $T =$ 230 K to 0.73 atm cm^2 s^{-1} at $T = 320$ K. These corrections on the measured values of k_1' were less than 5%. Examples of the pseudo-first-order plots measured from the BrO decay kinetics at different temperatures are shown in Figure 5. The 0-intercepts, in the range of 2 ± 5 s^{-1} under the temperature conditions of the study, are in good agreement with the BrO loss rates measured in the absence of HO_2, 3 ± 2 s^{-1}. The results for k_1 from this series of experiments are reported in Table 1.

HO_2 Kinetics in Excess BrO. In this series of experiments, reaction 1 was studied under pseudo-first-order conditions using an excess of BrO over HO_2 radicals. HO_2 radicals, formed in the reaction of F atoms (inlet 1) with excess H_2O_2 (inlet 2), were introduced into the reactor through the central tube of the movable injector. BrO radicals were produced from the reaction of Br atoms (from the discharge of Br_2 or a Br_2/O_2 mixture, inlet 3) with ozone, which was introduced into the reactor through its sidearm (inlet 4). The reaction of oxygen atoms (inlet 3) with an O_3/Br_2 mixture (inlet 4) was also used to produce BrO radicals. The initial concentrations of HO_2 and BrO radicals are shown in Table 1. Rather high initial concentrations of HO_2 were used in order to reduce the relative contribution from $O^{16}O^{17+}$ ions (from O_2/O_3, see previous section) to the HO_2 signal at $m/e = 33$. The concentrations of the precursor species in the reactor were as follows: $[H_2O_2] = (0.7-1.3) \times 10^{13}$, $[O_3] = (1.5-2.0) \times 10^{14}$, and $[Br_2] \approx 10^{14}$ molecule cm^{-3}. Linear flow velocities were in the range of 1540−1790 cm s^{-1}. The consumption of the excess reactant, BrO radicals (up to 20% of its initial concentration), was observed. This BrO consumption, due to reaction 1, to the BrO wall loss, and to the BrO disproportionation reaction 14, was taken into account using the mean concentration of the radicals over the whole reaction time. The pseudo-first-order rate constants, $k_1' = -$d(ln-[HO_2])/dt, obtained from the HO_2 consumption kinetics were also corrected for the axial and radial diffusion of HO_2. The diffusion coefficient of HO_2 in He was calculated from that of O_2 in He[22] and varied from 0.52 atm cm^2 s^{-1} at $T = 243$K to 1.03 atm cm^2 s^{-1} at $T = 360$ K. The corrections on the values of k_1' were less than 10%. The possible impact of the secondary and side reactions on the observed kinetics of HO_2 consumption must be discussed. First, the Br atoms present in the reactor could react with HO_2 through reaction 19. Br concentrations are at steady state, which is defined mainly by Br production through reaction 14a and consumption through reaction 5 with ozone. Considering that, under the experimental conditions used, (i) [Br] is a few times lower than [BrO] and (ii) $k_1/k_{19} = 12-33$, the contribution of reaction 19 to the HO_2 decay can be disregarded. Another species potentially influencing the observed kinetics of HO_2 is OH, which could be produced in the source of HO_2 via reaction 8 of F atoms with H_2O. OH radicals, if present in the reactor, could lead either to the formation of HO_2 in reaction 2 or to the additional consumption of HO_2 through reaction 21.

$$OH + HO_2 \rightarrow H_2O + O_2 \qquad (21)$$

$$k_{21} = 4.8 \times 10^{-11} \exp(250/T) \text{ cm}^3 \text{ molecule}^{-1} \text{ s}^{-1}$$ [18]

To reduce the role of the OH-initiated chemistry in the present experiments, Br_2 ($\sim 10^{14}$ molecule cm^{-3}) was added into the reactor, resulting in efficient OH scavenging through reaction 10. The validity of this procedure was checked at $T = 298$K in the following way. The measurements of k_1 were carried out under different experimental conditions: with low $[Br_2]$ ($\sim 10^{12}$ molecule cm^{-3}) and relatively high initial concentration of OH radicals ($[OH] = 0.25 \times [HO_2]_0$) and with high $[Br_2]$ ($\sim 10^{14}$ molecule cm^{-3}) and low initial concentration of OH ($< 0.03 \times [HO_2]_0$). The initial concentration of OH radicals could be measured by scavenging OH radicals with an excess of Br_2 with subsequent detection of HOBr (as explained in the previous section). The pseudo-first-order plots obtained from the HO_2 decay kinetics under these experimental conditions are shown in Figure 6. One can note that the OH-initiated chemistry leads to an underestimation of k_1 under the experimental conditions used. The difference between the values of k_1 resulting from the two fits presented in Figure 6 is around 25%. Further, a numerical simulation of the HO_2 kinetics observed in the presence of OH in the reactor has been performed. The rate constant of reaction 1 was found from the best fit to the HO_2 decay kinetics using the experimental profiles of [BrO] and a mechanism including reaction 1; HO_2 wall loss; and the reactions of OH with Br_2 (10), BrO (2), and HO_2 (21). The corrected values of k_1' obtained in this way are also shown in Figure 6. They are in excellent agreement with the results

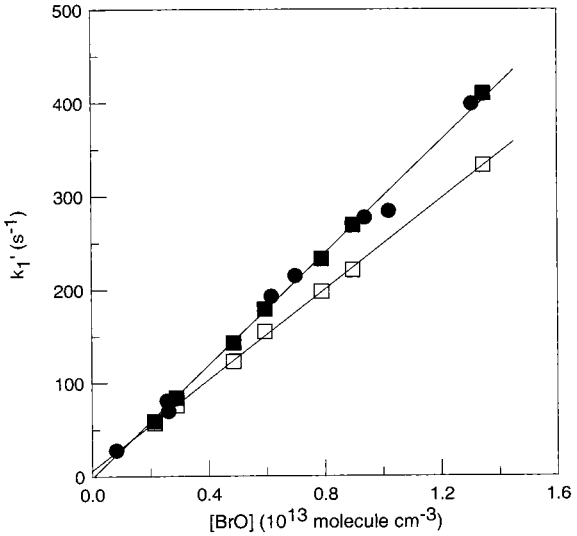

Figure 6. Reaction $HO_2 + BrO \rightarrow HOBr + O_2$ (1): pseudo-first-order plot obtained from HO_2 decay kinetics in excess BrO at $T = 298$ K. □ = measured in the presence of OH, ■ = corrected for OH-initiated chemistry, ● = measured in absence of OH (see text).

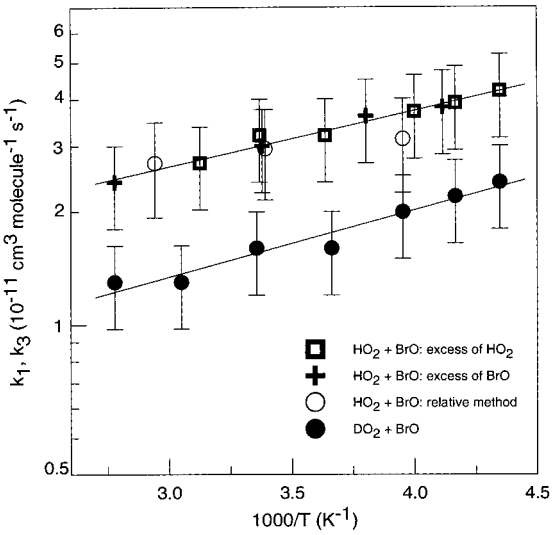

Figure 7. Reactions $HO_2 + BrO \rightarrow HOBr + O_2$ (1) and $DO_2 + BrO \rightarrow DOBr + O_2$ (3): temperature dependence of the rate constants.

obtained in the OH-free system. All of the results obtained for k_1 at different temperatures in this series of experiments are reported in Table 1. These results are also shown in Figure 7, together with those obtained from the monitoring of BrO decays in an excess of HO_2 radicals. One can note the good agreement between the values of k_1 obtained under the different experimental conditions.

The uncertainties in k_1 shown in Figure 7 represent a 25% conservative uncertainty, which is a combination of statistical and estimated systematic errors. The estimated systematic uncertainties include ±5% for flow meter calibrations, ±1% for temperature, ±3% for pressure, and ±15% for the procedure of measuring the absolute concentrations of the radicals. Combining these uncertainties in quadrature and adding 2σ (∼10%) statistical uncertainty (see Table 1), yields ∼25% overall uncertainty in the values of k_1. The straight line in Figure 7, resulting from the least-squares analysis of all of these data, provides the Arrhenius expression

$$k_1 = (9.4 \pm 2.3) \times 10^{-12} \times \exp[(345 \pm 60)/T] \text{ cm}^3 \text{ molecule}^{-1} \text{ s}^{-1} \qquad T = 230-360 \text{ K}$$

where the quoted uncertainties represent 95% confidence limits and include estimated systematic errors.

Relative Measurements of k_1. In the relative study of reaction 1 using reaction 19 as the reference, the titration of the initial concentration of HO_2 radicals, $[HO_2]_0$, by a mixture of excess BrO and Br was carried out, and the yield of HOBr as a function of the [Br]/[BrO] ratio was measured. The concentration of HOBr formed was defined by the fraction of $[HO_2]_0$ reacting with BrO.

$$[\text{HOBr}] = \frac{k_1[\text{BrO}]}{k_1[\text{BrO}] + k_{19}[\text{Br}]}[\text{HO}_2]_0$$

Considering the derived expression

$$\frac{[\text{HO}_2]_0}{[\text{HOBr}]} - 1 = \frac{k_{19}}{k_1}\frac{[\text{Br}]}{[\text{BrO}]}$$

the ratio k_{19}/k_1, and hence k_1, can be obtained by plotting $([HO_2]_0/[HOBr] - 1)$ as a function of the [Br]/[BrO] ratio.

In these experiments, HO_2 radicals were produced in reaction 6 between F atoms and H_2O_2 in the central tube of the injector. Br and BrO were formed simultaneously by passing O_2/Br_2 mixtures (excess Br_2) through the microwave discharge (inlet 3). The [Br]/[BrO] ratio could be changed either by varying O_2 in the discharge or by adding ozone in the reactor (inlet 4).

It can be noted that the above method did not require absolute calibrations of the mass spectrometric signals of HO_2 and HOBr, as the initial concentration of HO_2 could be related to HOBr signal when $[HO_2]_0$ was completely converted to HOBr by reaction with excess BrO in the Br-free system (for high concentrations of ozone, $[O_3] \approx 5 \times 10^{14}$ molecule cm^{-3}). Thus, only HOBr signals were recorded, first in the Br-free system, corresponding to $[HO_2]_0$, and second in the Br and BrO containing system, corresponding to the fraction of $[HO_2]_0$ that reacted with BrO. The concentration of OH from the source of HO_2 was verified to be too low ($[OH] < 0.03[HO_2]_0$) to influence the results of these experiments through HOBr and HO_2 formation in reactions 10 and 2, respectively. The initial concentration of HO_2 radicals was around 10^{12} molecule cm^{-3}. The Br and BrO concentration ranges are shown in Table 2. The reported values are the mean concentrations used in the calculations, as the changes in [Br] and [BrO] (within 20%) were observed on the time scale of the HO_2 titration experiments (∼10^{-2} s). In fact, the BrO consumption in the fast (at high BrO concentrations) disproportionation reaction of BrO radicals (14) was compensated by the BrO regeneration in the Br reaction with ozone, leading to steady states for [Br] and [BrO]. Increasing the reaction time did not lead to changes in the HOBr signal, demonstrating that HO_2 was completely consumed in the reactions with Br and BrO under the experimental conditions used. All of the data obtained at the three temperatures of the relative measurement study are presented in Figure 8. According to the expression given above, the slopes of the linear dependencies in Figure 8 give the k_{19}/k_1 ratio at each temperature. The results thus obtained are presented in Table 2, which also reports the calculated values of k_1. The values of k_{19} needed for these calculations were derived from the Arrhenius expression $k_{19} = 4.9 \times 10^{-12} \exp(-310/T)$ cm^3 molecule^{-1} s^{-1},[16] with addition of a conservative 15% uncertainty. The values of k_1 resulting from these relative measurements are also shown in Figure 7.

TABLE 2: Reaction $HO_2 + BrO \rightarrow HOBr + O_2$ (1): Relative Measurements of the Rate Constant

T (K)	$[Br]^a/10^{14}$	$[BrO]^a/10^{13}$	[Br]/[BrO]	k_{19}/k_1	$k_{19}{}^b/10^{-12}$	$k_1{}^b/10^{-11}$
340	0.3−1.1	0.3−2.5	2.2−35.9	0.073 ± 0.010	1.97 ± 0.30	2.70 ± 0.77
295	0.6−1.4	0.3−3.1	2.0−46.7	0.058 ± 0.007	1.71 ± 0.26	2.95 ± 0.80
253	0.7−1.5	0.4−3.1	2.1−31.6	0.046 ± 0.006	1.44 ± 0.22	3.13 ± 0.88

[a] Concentrations are in units of molecule cm^{-3}. [b] Rate constants are in units of cm^3 molecule^{-1} s^{-1}.

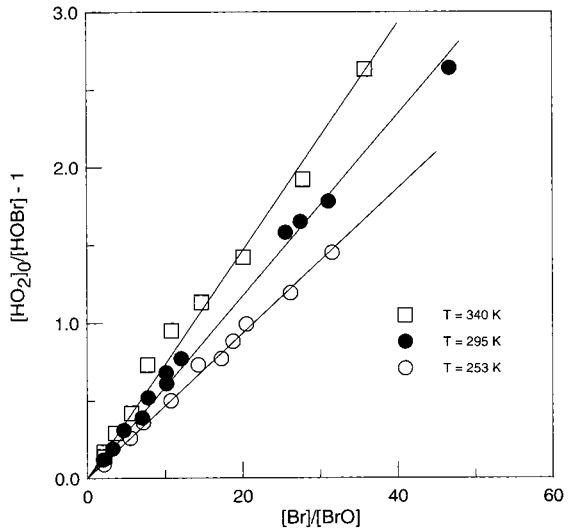

Figure 8. Reaction $HO_2 + BrO \rightarrow HOBr + O_2$ (1): relative measurements of the rate constant (see text).

They are in good agreement with the results of the direct measurements of k_1 obtained in this study (however, these data were not used in the above determination of the Arrhenius expression for k_1).

Reaction $BrO + HO_2 \rightarrow$ Products: Mechanistic Study. To determine the branching ratio for the HBr and O_3 forming channel of reaction 1 additional experiments were performed, consisting of a chemical titration of the relatively high concentration of BrO by an excess of HO_2, with subsequent detection of ozone possibly formed in channel 1b. Experiments were carried out at room temperature ($T = 298$K). HO_2 radicals were produced in the central tube of the movable injector by reaction of F atoms with H_2O_2. BrO radicals were formed in reaction 4 between oxygen atoms (inlet 3) and excess Br_2 molecules (inlet 4). The concentrations of Br_2 and H_2O_2 in the reactor were 5×10^{13} and 4×10^{13} molecule cm^{-3}, respectively. HOBr, the main product of reaction 1, was also detected, and the branching ratio for the O_3 formation channel could be found as $\Delta[O_3]/\Delta[HOBr]$ (assuming that $k_{1a} \approx k_1$). With initial concentrations of 8.5×10^{12} and 5×10^{12} molecule cm^{-3}, respectively, for HO_2 and BrO, the formation of 4.15×10^{12} molecule cm^{-3} of HOBr for 4.1×10^{12} molecule cm^{-3} of consumed BrO was observed at a reaction time of $\sim 10^{-2}$s. The formation of ozone at measurable concentrations was not observed. $[O_3]$ was estimated to be less than 1.1×10^{10} molecule cm^{-3} under these experimental conditions. This led to the determination of the upper limit for the branching ratio of the O_3 forming channel: $k_{1b}/k_1 \leq 2.7 \times 10^{-3}$. Br atoms, formed in the BrO source via reactions 4 and 14, were observed in the reactor at concentrations of ca. 10^{13} molecule cm^{-3}. A correction on k_{1b}/k_1 for possible O_3 consumption in the reaction with Br atoms was made, leading to the final value of $k_{1b}/k_1 \leq 3.2 \times 10^{-3}$. Finally, the upper limit for the branching ratio of channel 1b recommended from this study is

$$k_{1b}/k_1 < 4 \times 10^{-3} \quad \text{at } T = 298 \text{ K}$$

The experimental determination of such an extremely low upper limit for the branching ratio k_{1b}/k_1 could be achieved mainly through the use of high initial concentrations of both reactants. The simultaneous formation of HO_2 and BrO at such high concentrations was not possible at low temperatures. Consequently, these experiments were limited to room temperature.

Rate Constant for the $BrO + DO_2$ Reaction. The rate constant of reaction 3 was measured similarly to that of the $BrO + HO_2$ reaction. The kinetics of DO_2 consumption were monitored in an excess of BrO radicals. DO_2 radicals were formed in the reaction of F atoms with excess D_2O_2 in the central tube of the movable injector. BrO radicals were produced in the reactor through the reaction of O atoms (from discharge of O_2/He, inlet 3) with Br_2/O_3 mixture (inlet 4). The initial concentrations of DO_2 radicals were in the range $(0.8-1.2) \times 10^{12}$molecule cm^{-3}. These relatively high initial concentrations of DO_2 were used in order to reduce the relative contribution from $O^{16}O^{18+}$ ion to the DO_2 signal at $m/e = 34$. The concentrations of the precursor species in the reactor were as follows: $[D_2O_2] = (6-8) \times 10^{12}$, $[O_3] = (1.5-2.0) \times 10^{14}$, and $[Br_2] \approx 10^{14}$ molecule cm^{-3}. The pseudo-first-order rate constants, $k_1' = -d(\ln[DO_2])/dt$, obtained from the DO_2 consumption kinetics were corrected for the axial and radial diffusion of DO_2. The diffusion coefficient of DO_2 in He was calculated from that of O_2 in He[22] and varied from 0.48 atm cm^2 s^{-1} at $T = 230$ K to 1.02 atm cm^2 s^{-1} at $T = 360$ K The maximal correction to the measured values of k_1' was around 10%. Similarly to the study of reaction 1, the possible influence of the secondary chemistry initiated by OD radicals (from the DO_2 source) was minimized through the presence of high $[Br_2]$ in the reactor, leading to OD scavenging via reaction 11. It can be also noted that the rate constant for the $OD + DO_2$ reaction is about 3 times lower than that of the $OH + HO_2$ reaction.

$$OD + DO_2 \rightarrow D_2O + O_2 \qquad (22)$$

$$k_{22} = 3.7 \times 10^{-11} \text{ cm}^3 \text{ molecule}^{-1} \text{ s}^{-1} \quad \text{at } T = 298\text{K}$$

(unpublished data from this laboratory).

Br atoms, originating from the BrO source, were present in the reactor and could react with DO_2 through reaction 23.

$$DO_2 + Br \rightarrow DBr + O_2 \qquad (23)$$

$$k_{23} = 1.9 \times 10^{-12} \exp(-540/T) \text{ cm}^3 \text{ molecule}^{-1} \text{ s}^{-1}$$ [16]

However, the contribution of this reaction to DO_2 consumption could be disregarded considering that, under the experimental conditions of the study, (i) the Br concentration was always lower than that of BrO by a factor 2−5 and (ii) $k_3/k_{23} = 60-230$ in the temperature range used. Examples of the pseudo-first-order plots obtained from the DO_2 decay kinetics are shown in Figure 9. All of the results obtained for k_3 at the different temperatures of the study are reported in Table 3. The temperature dependence of the rate constant of reaction 3 is also shown in Figure 7. The error bars shown for k_3 represent conservative 25% uncertainty, which includes statistical and estimated systematic errors. These data provide the Arrhenius

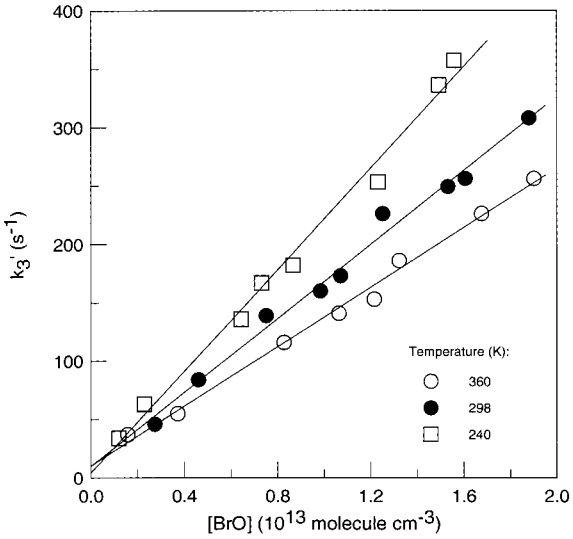

Figure 9. Reaction $DO_2 + BrO \rightarrow DOBr + O_2$ (3): examples of pseudo-first-order plots obtained from DO_2 decay kinetics in excess BrO at different temperatures.

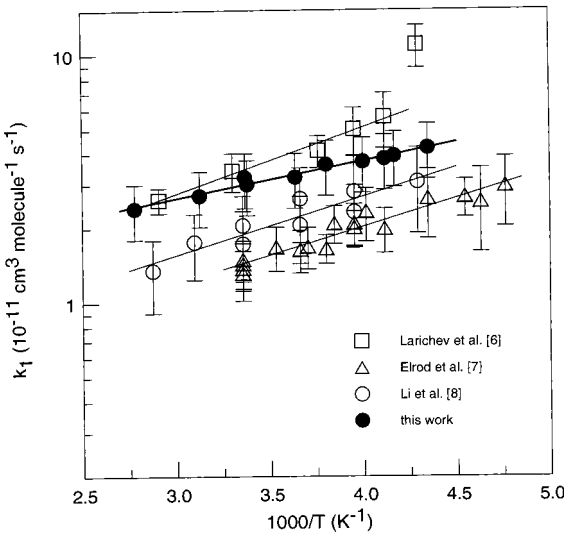

Figure 10. Reaction $HO_2 + BrO \rightarrow HOBr + O_2$ (1): summary of the results from the temperature dependence studies.

TABLE 3: Reaction $DO_2 + BrO \rightarrow DOBr + O_2$ (3): Experimental Conditions and Results

N/exp[a]	T (K)	[BrO][b]	k_3[c]
8	360	1.6−19.0	1.3 ± 0.1
8	328	1.2−19.8	1.3 ± 0.1
9	298	2.7−18.8	1.6 ± 0.1
8	273	1.7−15.3	1.6 ± 0.2
8	253	1.5−16.4	2.0 ± 0.2
8	240	1.2−15.6	2.2 ± 0.2
6	230	1.4−9.5	2.4 ± 0.3

[a] Number of kinetic runs. [b] Concentrations are in units of 10^{12} molecule cm^{-3}. [c] Rate constants are in units of 10^{-11} cm^3 $molecule^{-1}$ s^{-1}; the error represents $\pm 2\sigma$.

expression

$$k_3 = (3.9 \pm 1.2) \times 10^{-12} \times \exp[(410 \pm 80)/T] \text{ cm}^3 \text{ molecule}^{-1} \text{ s}^{-1} \qquad T = 230-360 \text{ K}$$

where the quoted uncertainties represent 95% confidence limits and include estimated systematic errors.

Discussion

The results obtained for the rate constant of the $HO_2 + BrO$ reaction can be compared with those from previous studies. A summary of all of the data available for k_1 is presented in Table 4. The results of the temperature dependence studies are also shown in Figure 10. Although a negative temperature dependence of the rate constant is observed, similarly to the previous studies,[6−8] the activation energy determined in the present work is slightly lower than those previously reported: $E/R = 345$ K compared with 520−580 K.[6−8] The present determination of k_1 is in good agreement with previous data from this laboratory,[6] especially at room and higher temperatures (see Figure 10). The difference between the results of the two studies at low temperatures can be explained by the heterogeneity complications observed and discussed in ref 6. Heterogeneity problems were especially pronounced at the lowest temperature of the previous study (233 K), leading to an abnormally high value measured for k_1, but such problems could also occur to a lesser extent for $T > 233$ K. Under the experimental conditions of the present study, heterogeneity complications were not observed. The room-temperature value of k_1 obtained in the present work is in good agreement with those measured by Bridier et al.[5] and Larichev et al.[6] and is significantly higher than those from the most recent studies[7−9] (see Table 4). Although the same equipment was used, the present investigation differs from the previous one from this group.[6] First, reaction 6 between F and H_2O_2 was used in the present work to produce HO_2 radicals instead of the $Cl + CH_3OH$ (+ O_2) reaction, which was employed in ref 6 and which is known to be strongly affected by wall processes. Second, another configuration of the movable injector was used for the production of the radicals and their introduction into the reactor. In the present study, the two microwave discharge cavities used for the production of the

TABLE 4: Reaction $BrO + HO_2 \rightarrow HOBr + O_2$ (1): Summary of the Measurements of the Rate Constant

reference	technique[a]	pressure (Torr)	T (K)	k_1 (10^{-11} cm^3 $molecule^{-1}$ s^{-1})	
				$k_1 = f(T)$	k_1(298K)
Cox and Sheppard[4]	MP/UV	760	303		$0.5^{+0.5}_{-0.3}$
Poulet et al.[2]	DF/MS	1	298		3.3 ± 0.5
Bridier et al.[5]	FP/UV	760	298		3.4 ± 1.0
Larichev et al.[6]	DF/MS	1	233−344	$(0.48 \pm 0.03) \exp(580 \pm 100/T)$	3.3 ± 0.5
Elrod et al.[7]	DF/MS	100	210−298	$(0.25 \pm 0.08) \exp(520 \pm 80/T)$	1.4 ± 0.3
Li et al.[8]	DF/MS	1	233−348	$(0.31 \pm 0.03) \exp(540 \pm 210/T)$	1.73 ± 0.61[b] 2.05 ± 0.64[c]
Cronkhite et al.[9]	LFP/UV/TDLAS	12, 25	296		2.0 ± 0.6
this work	DF/MS	1	230−360	$(0.94 \pm 0.23) \exp(345 \pm 60/T)$	3.2 ± 0.8[b] 3.0 ± 0.8[c]

[a] MP/UV = modulated photolysis/UV absorption; DF/MS = discharge flow/mass spectrometry; FP/UV = flash photolysis/UV absorption; LFP/UV/TDLAS = laser flash photolysis/UV absorption/tunable diode laser absorption. [b] HO_2 in excess. [c] BrO in excess.

active species were located on the movable injector. This allowed the injection of both radicals, HO_2 and BrO, through the movable inlet, leading to the elimination of problems associated with the loss of radicals on the outer surface of the injector, which occurs when radicals are introduced through the reactor sidearm. In the present work, k_1 was measured either from the monitoring of HO_2 decays in excess BrO or from the monitoring of the BrO consumption kinetics in excess HO_2. The concentrations of the excess reactants were varied widely. The results obtained for k_1 with these two different experimental approaches were in very good agreement. Finally, independent relative measurements of k_1 were also conducted in the present work. The main goal of the relative measurements was to investigate whether the values of k_1 determined in this way were closer to 3×10^{-11}, as measured in this study, or to 2×10^{-11} cm^3 $molecule^{-1}$ s^{-1}, as reported by the other studies.[7−9] The results obtained for k_1 ($\sim 3 \times 10^{-11}$ cm^3 $molecule^{-1}$ s^{-1}) by this relative method agree well with the absolute values from the present work. In conclusion, the present study does not resolve the problem of the existing discrepancy in k_1 at room temperature, supporting the "high" values of k_1, measured previously in refs 2, 5, and 6, although the present result overlaps those from refs 8 and 9 if the quoted uncertainties are considered (Table 4). Current evaluation of the kinetic data for atmospheric modeling[18] recommends the following expression for k_1: $k_1 = 3.4 \times 10^{-12} \exp[-(540 \pm 200)/T]$ cm^3 $molecule^{-1}$ s^{-1}. One can note that the Arrhenius expression from the present work results in only slightly higher values for k_1 at stratospheric temperatures: by a factor of 1.1−1.25 at temperatures in the range 210−250 K.

The present determination of the rate constant for reaction 3 between BrO and DO_2 appears to be the first. A moderate kinetic isotopic effect is observed for $HO_2(DO_2)$ + BrO reactions. A ratio $k_1/k_3 \approx 2$ has been found at the temperatures of the present study. This effect is due to the lower preexponential factor in k_3, as comparable values were found for the activation energies of reactions 1 and 3.

Current photochemical models, which consider HBr production only through gas-phase reactions of Br with HO_2 and CH_2O, fail to reproduce the results of recent observations of around 1−2 ppt of HBr in the altitude range 20−35 km [e.g., ref 23]. The models generally underestimate the stratospheric concentrations of HBr. Reaction 1b has been proposed as one of the potential candidates for additional HBr formation in the stratosphere. It has been also shown that a branching ratio of 0.01 for the HBr + O_3 forming channel of reaction 1 could lead to a reasonable agreement between observed and calculated stratospheric HBr profiles.[3] In this respect, the value of $k_{1b}/k_1 < 0.004$ measured in the present study at $T = 298$ K, seems to exclude this possibility, assuming that this value can be applied at low temperatures. This assumption seems to be reasonable, as the low values for k_{1b}/k_1 measured in the present study and in ref 10 can probably be considered as an indication of the existence of a significant barrier for HBr elimination from the HOOOBr intermediate complex. Another potential source of the stratospheric HBr is the minor channel 2b of the reaction between OH and BrO radicals, which is presently under investigation.

Acknowledgment. This study was carried out within a project funded by the European Commission within the Environment and Climate Program (contract COBRA-ENV-CT97-0576).

References and Notes

(1) Yung, Y. L.; Pinto, J. P.; Watson, R. T.; Sander, S. P. *J. Atmos. Sci*. **1980**, *37*, 339.
(2) Poulet G.; Pirre, M.; Maguin, F.; Ramoroson, R.; Le Bras, G. *Geophys. Res. Lett.* **1992**, *19*, 2305.
(3) Chartland, D. J.; McConnell, J. C. *Geophys. Res. Lett.* **1998**, *25*, 55.
(4) Cox, R. A.; Sheppard, D. W. *J. Chem. Soc., Faraday Trans. 2* **1982**, *78*, 1383.
(5) Bridier, I.; Veyret, B.; Lesclaux, R. *Chem. Phys. Lett.* **1993**, *201*, 563.
(6) Larichev, M.; Maguin, F.; Le Bras G.; Poulet, G. *J. Phys. Chem.* **1995**, *99*, 15911.
(7) Elrod, M. J.; Meads, R. F.; Lipson, J. B.; Seeley, J. V.; Molina, M. J. *J. Phys. Chem.* **1996**, *100*, 5808.
(8) Li, Z.; Friedl, R. R.; Sander, S. P. *J. Chem. Soc., Faraday Trans.* **1997**, *93*, 2683.
(9) Cronkhite, J. M.; Stickel, R. E.; Nicovich, J. M.; Wine, P. H. *J. Phys. Chem. A* **1998**, *102*, 6651.
(10) Mellouki, A.; Talukdar, R. K.; Howard, C. J. *J. Geophys. Res.* **1994**, *99*, 22949.
(11) Chipperfield, M. P.; Shallcross, D. E.; Lary, D. J. *Geophys. Res. Lett.* **1997**, *24*, 3025.
(12) Bogan, D. J.; Thorn, R. P.; Nesbitt, F. L.; Stief, L. J. *J. Phys. Chem.* **1996**, *100*, 14383.
(13) Bedjanian, Y.; Le Bras, G.; Poulet, G. *J. Phys. Chem*. **1999**, *103*, 7017.
(14) Bedjanian, Y.; Le Bras, G.; Poulet, G. *Int. J. Chem. Kinet.* **1999**, *31*, 698.
(15) Bedjanian, Y.; Riffault, V.; Le Bras, G.; Poulet, G. *J. Photochem. Photobiol. A: Chem.* **1999**, *128*, 15; *J. Phys. Chem.* **1999**, *103*, 7017.
(16) Bedjanian, Y.; Riffault, V.; Le Bras, G.; Poulet, G. *J. Phys. Chem*. **2001**, *105*, 573.
(17) Nicovich, J. M.; Wine, P. H. *Int. J. Chem. Kinet.* **1990**, *22*, 379.
(18) De More, W. B.; Sander, S. P.; Golden, D. M.; Hampson, R. F.; Kurylo, M. J.; Howard, C. J.; Ravishankara, A. R.; Kolb, C. E.; Molina, M. J. *Chemical Kinetics and Photochemical Data for Use in Stratospheric Modeling*; NASA, JPL, California Institute of Technology: Pasadena, CA, 1997.
(19) Walther, C. D.; Wagner, H. G. *Ber. Bunsen-Ges. Phys. Chem.* **1983**, *87*, 403.
(20) Bemand, P. P.; Clyne, M. A. A. *J. Chem. Soc., Faraday Trans. 2* **1976**, *72*, 191.
(21) Kaufman, F. *J. Phys. Chem.* **1984**, *88*, 4909.
(22) Morrero, T. R.; Mason, E. A. *J. Phys. Chem. Ref. Data* **1972**, *1*, 3.
(23) Nolt, I. G.; Ade, P. A. R.; Alboni, F.; Carli, B.; Carlotti, M.; Cortesi, U.; Epifani, M.; Griffin, M. J.; Hamilton, P. A.; Lee, C.; Lepri, G.; Mencaraglie, F.; Murray, A. G.; Park, J. H.; Raspollini, P.; Ridolfi, M.; Vanek, M. D. *Geophys. Res. Lett*. **1997**, *24*, 281.